The EMBO Journal Vol. 21 No. 24 pp. 6689–6699, 2002

Myosin VIIa, harmonin and cadherin 23, three Usher I gene products that cooperate to shape the sensory hair cell bundle

Batiste Boëda, Aziz El-Amraoui, Amel Bahloul[1], Richard Goodyear[2], Laurent Daviet[3], Stéphane Blanchard, Isabelle Perfettini, Karl R.Fath[4,5], Spencer Shorte[6], Jan Reiners[4], Anne Houdusse[1], Pierre Legrain[3], Uwe Wolfrum[4], Guy Richardson[2] and Christine Petit[7]

Unité de Génétique des Déficits Sensoriels, CNRS URA 1968 and [6]Centre d'Imagerie Dynamique, Institut Pasteur, 25 rue du Dr Roux, 75724 Paris cedex 15, [1]UMR 144 CNRS/IC, Institut Curie, 26 rue d'Ulm, 75248 Paris cedex 05 and [3]Hybrigenics, 3–5 impasse Reille, 75014 Paris, France, [2]School of Biological Sciences, The University of Sussex, Falmer, Brighton BN1 9QG, UK and [4]Institut für Zoologie, Johannes Gutenberg-Universität Mainz, D-55099 Mainz, Germany

[5]Present address: Queens College of CUNY, 65–30 Kissena Blvd, Flushing, NY 11367, USA

[7]Corresponding author
e-mail: cpetit@pasteur.fr

B.Boëda and A.El-Amraoui contributed equally to this work

Deaf-blindness in three distinct genetic forms of Usher type I syndrome (USH1) is caused by defects in myosin VIIa, harmonin and cadherin 23. Despite being critical for hearing, the functions of these proteins in the inner ear remain elusive. Here we show that harmonin, a PDZ domain-containing protein, and cadherin 23 are both present in the growing stereocilia and that they bind to each other. Moreover, we demonstrate that harmonin b is an F-actin-bundling protein, which is thus likely to anchor cadherin 23 to the stereocilia microfilaments, thereby identifying a novel anchorage mode of the cadherins to the actin cytoskeleton. Moreover, harmonin b interacts directly with myosin VIIa, and is absent from the disorganized hair bundles of myosin VIIa mutant mice, suggesting that myosin VIIa conveys harmonin b along the actin core of the developing stereocilia. We propose that the shaping of the hair bundle relies on a functional unit composed of myosin VIIa, harmonin b and cadherin 23 that is essential to ensure the cohesion of the stereocilia.

Keywords: cadherin 23/hair bundle/harmonin/myosin VIIa/Usher syndrome

Introduction

Usher syndrome (USH) is the most frequent cause of deaf-blindness in humans. Three clinical subtypes, USH1–3, have been described (reviewed in Petit, 2001). USH1 is the most severe form. It is characterized by severe to profound congenital sensorineural deafness, constant vestibular dysfunction (balance deficiency) and pre-pubertal onset retinitis pigmentosa. USH1 is genetically heterogeneous. Evidence for seven distinct genetic loci (*USH1A–G*) has been obtained, and four of the corresponding genes have been identified, namely *USH1B*, *C*, *D* and *F* (Petit, 2001; Mustapha *et al*., 2002). *USH1B* encodes the actin-based motor protein myosin VIIa (Weil *et al*., 1995). *USH1C* encodes harmonin (Bitner-Glindzicz *et al*., 2000; Verpy *et al*., 2000), a protein that contains PDZ domains (postsynaptic density, disc large, zonula occludens), modules known as organizers of submembranous protein complexes (Sheng and Sala, 2001). Alternatively spliced *USH1C* transcripts (Verpy *et al*., 2000) predict at least 10 protein isoforms which can be grouped into three subclasses, hereafter referred to as harmonin a, b, and c, and collectively as harmonin (Figure 1A). Finally, mutations in the genes encoding two cadherin-related proteins, cadherin 23 and protocadherin 15, underlie USH1D (Bolz *et al*., 2001; Bork *et al*., 2001) and USH1F (Ahmed *et al*., 2001; Alagramam *et al*., 2001a), respectively.

Mouse mutants defective for myosin VIIa (*shaker-1*) (Mburu *et al*., 1997), cadherin 23 (*waltzer*) (Di Palma *et al*., 2001) and protocadherin 15 (*Ames waltzer*) (Alagramam *et al*., 2001b) have been reported. They are all deaf and exhibit vestibular dysfunction. In these mutants, the sensory cells of the cochlea (the auditory organ) and vestibular end organs (balance organs) display anomalies in the development of their hair bundle. This mechanosensory structure is composed of an ensemble of 30–300 microvilli called stereocilia, that project from the apical surface of the hair cell (DeRosier and Tilney, 2000) (Figure 1B). As in other microvilli, stereocilia are tightly packed with actin filaments that are uniformly polarized and have their barbed end, i.e. their faster growing end, located at the tip (DeRosier and Tilney, 2000). However, stereocilia have several specific morphological features: (i) they are wider and longer than the microvilli of 'conventional' epithelial cells and can contain up to 2000 actin filaments in some species; (ii) they taper off at their base, where they insert into the apical surface of the cell, with only a few centrally located actin filaments extending through this region to anchor them into the cuticular plate (Figure 1B, right panel), a dense meshwork of cross-linked actin filaments (DeRosier and Tilney, 1989); (iii) they are packed into rows of increasing height to form a highly organized and uniformly oriented hair bundle (Figure 1B); and (iv) they are connected by several different types of extracellular links (Pickles *et al*., 1984; Goodyear and Richardson, 1999). Upon deflection in response to the sound or acceleration stimulus, the stereocilia all pivot around their basal insertion points, causing opening or closing of the transduction channels, and thus fluctuations in the cell's membrane potential (Hudspeth, 1997).

With the exception of some studies addressing the role of myosin VIIa (Gale *et al*., 2001; Tuxworth *et al*., 2001;

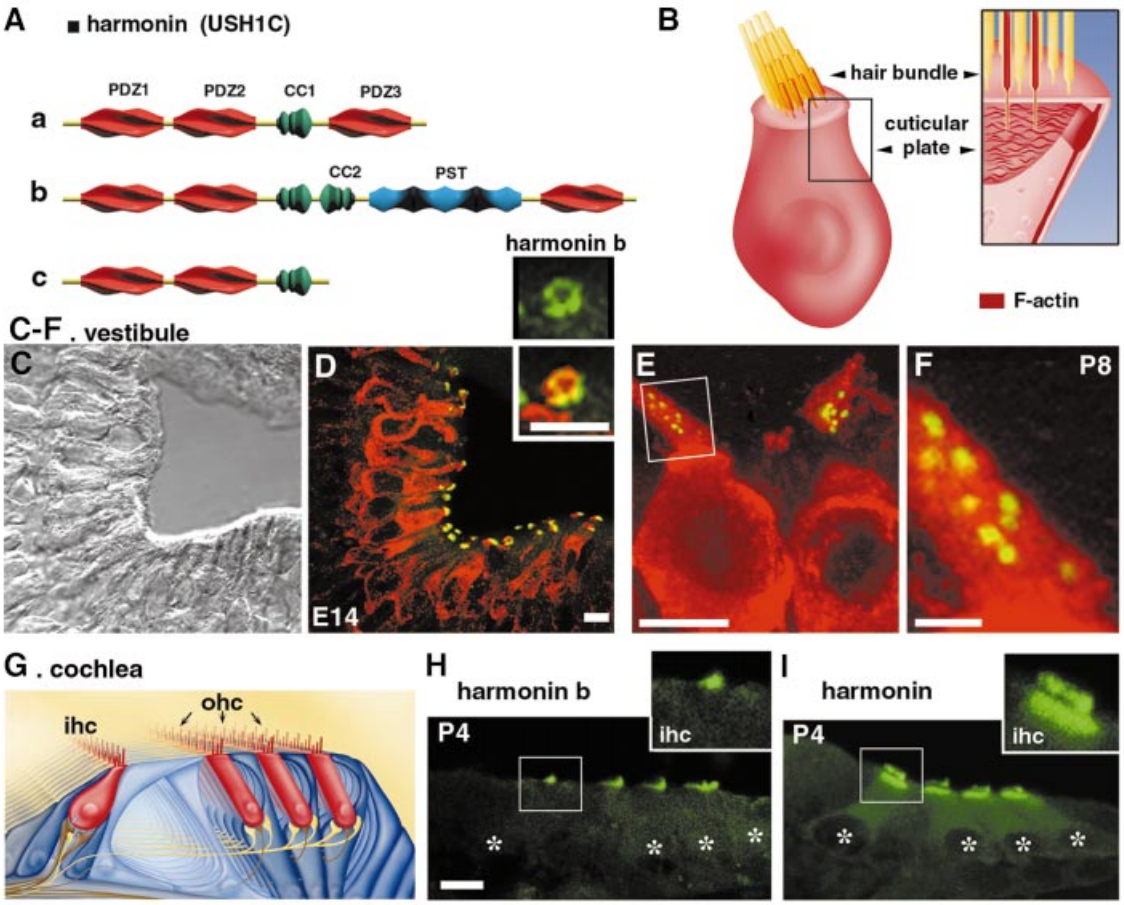

Fig. 1. (**A**) Predicted structures of harmonin a, b and c isoforms. Class a isoforms contain three PDZ domains and one coiled-coil (CC1) domain. The longest isoforms are grouped into class b; they contain an additional coiled-coil domain (CC2), and a proline, serine, threonine (PST)-rich region. Class c isoforms are the shortest; they contain only the first two PDZ domains and the first coiled-coil domain. (**B**) Schematic representation of an inner ear sensory hair cell. At the apical surface of the hair cell, a number of microvilli-like structures, called stereocilia, form the hair bundle. Each stereocilium contains a core of actin filaments (shown in red in the right panel). The central actin filaments of all the stereocilia insert into the cuticular plate, i.e. a dense meshwork of actin filaments lying beneath the apical cell surface. (C–F) Harmonin b in the vestibular hair cells (mouse). (**C** and **D**) At E14, harmonin b isoforms are only detected at the apical surface of the hair cells, whereas myosin VIIa staining delineates the whole cells. In a few cells, harmonin b immunoreactivity appears as a circle of bead-like foci located around the periphery of the cuticular plate (D and insets). At P8, harmonin b is located at the tips of the stereocilia (**E**, and detail in **F**), whereas myosin VIIa is present in both the hair cell bodies and stereocilia (E and F). (G–I) Harmonin in the cochlear hair cells (rat). (**G**) Schematic representation of the cochlear auditory organ (organ of Corti). It is made up of sensory cells (in red), namely the single row of inner hair cells (ihc) and the three rows of outer hair cells (ohc), and various types of supporting cells (in blue). (**H** and **I**) Distribution of harmonin isoforms in the rat organ of Corti at P4. Harmonin b is only detected in the hair bundle (H) of the sensory cells whereas, using the NW2 pan-harmonin antibody, harmonin isoforms a, b and c are detected in the cuticular plate as well as in the apical hair bundle (I). Asterisks indicate hair cell bodies. Bars: 10 μm in (C–E) and (H–I); and 5 μm in (F).

El-Amraoui *et al*., 2002; Kros *et al*., 2002), the functions of the proteins underlying USH1 remain elusive. Here we address the role of harmonin in the inner ear. Because the three aforementioned mouse models of USH1 have disorganized hair cell stereocilia, and because harmonin, within the inner ear, is restricted to the sensory cells (Verpy *et al*., 2000), we hypothesized that this protein also is involved in the development of a coherent hair bundle. This prompted us to seek molecular partners of this protein. Our results implicate harmonin, cadherin 23 and myosin VIIa in a single functional network that underlies the formation of a coherent hair cell bundle.

Results

Harmonin in differentiating hair cell stereocilia

We studied the distribution of harmonin during the period of hair bundle differentiation in the mouse and rat. In the mouse, stereocilia sprout from the apical surface of vestibular and cochlear hair cells at E13 and E15, respectively (Nishida *et al*., 1998; Denman-Johnson and Forge, 1999). In the cochlea, hair cell differentiation proceeds from the base to the cochlear apex and, by P4–P6, the hair bundles reach their final adult shape (Nishida *et al*., 1998). A previous analysis of harmonin transcripts (see Figure 1A) has indicated that class b isoforms are restricted largely to the inner ear, whereas a and c forms have a much broader expression throughout the entire organism (Verpy *et al*., 2000). We thus focused our analysis on the b isoforms. Two polyclonal antibodies directed against the harmonin PST domain, that is only present in b isoforms, were generated. They both gave the same cellular distribution pattern. In the mouse vestibule, harmonin b was detected from E13 onwards, and it was restricted to the emerging stereocilia of the hair cells (Figure 1C and D). Detailed analysis by confocal

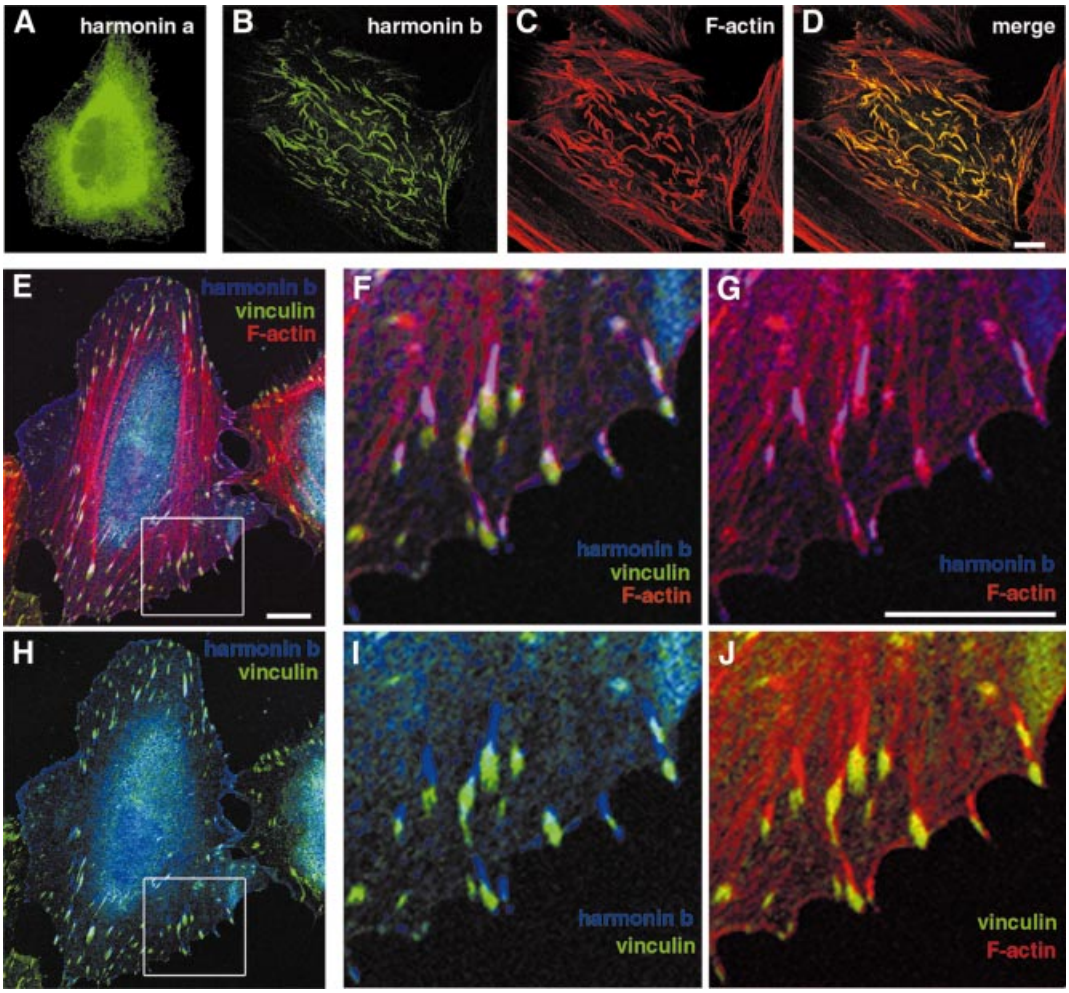

Fig. 2. Harmonin b induces F-actin bundling in HeLa cells. (A–D) HeLa cells were transiently transfected with either harmonin a (A) or harmonin b (B–D) cDNAs for 20 h. (**A**) Harmonin a is distributed throughout the cell body. (**B–D**) In contrast, overexpression of harmonin b (green) leads to the formation of harmonin b-immunoreactive long curvy bundles that co-localize with actin filaments (red). (**E–J**) HeLa cells transfected with harmonin b and collected 6 h after transfection. At this stage, most harmonin b labelling is present almost exclusively at the cell plasma membrane–substrate interface. A triple staining with rhodamine–phalloidin (red), anti-vinculin (green) and anti-harmonin b (blue) antibodies reveals that harmonin b decorates the extremities of actin stress fibres (violet in E–G). The enrichment of harmonin b labelling (blue) occurs close to the focal adhesion plaques visualized by anti-vinculin (green) staining (H–J). (F), (G), (I) and (J) are higher magnification views of the areas boxed in (E) and (H), respectively. Harmonin b and F-actin are both enriched at the distal ends of actin fibres (violet in F and G), and they slightly overlapped with the vinculin staining (I and J). Bars: 10 μm.

microscopy showed that between E13 and E16, the harmonin b labelling delineated the entire length of the stereocilia (not shown). Likewise in the cochlea, harmonin b was first detected at E15 in the differentiating hair bundles of the basal turn hair cells. From E15 to E17, the immunoreactivity extended towards the cochlear apex. From E16 in the vestibule (Supplementary figure 1A and B, available at *The EMBO Journal* Online) and P0 in the cochlea, the protein became concentrated at the apex of the maturing stereocilia (Figure 1E–I and data not shown). From P30 onwards, harmonin b was no longer detected in the cochlea. In the vestibule, the labelling only persisted in a few sensory hair cells, in both type I and type II hair cells (not shown). In contrast to the harmonin b expression profile, an antibody that recognizes an epitope common to the three harmonin isoform classes (a, b and c) detected the proteins both in the cuticular plate and along the stereocilia (Figure 1G–I), during the embryonic and postnatal life of the animal.

Harmonin b is an F-actin-bundling protein

To address the function of harmonin, a representative of each of the three isoform classes was first transfected into HeLa cells. In cells producing harmonin a (Figure 2A) or harmonin c (not shown), the protein was distributed uniformly throughout the cell body. In contrast, in cells expressing harmonin b, the protein was associated with filamentous structures (Figure 2B). Double immunolabels with antibodies to α-tubulin, β-tubulin, cytokeratin 18, vimentin or a pan cytokeratin antibody showed that harmonin b was not associated with microtubules or intermediate filaments (not shown). Rather, harmonin b was co-localized with actin filaments labelled with rhodamine–phalloidin (Figure 2B–D). To determine which domain(s) of harmonin b interact with the actin cytoskeleton, several truncated versions of the protein were expressed in HeLa cells. The shortest harmonin b fragment that co-localized with the actin filaments encompasses the second coiled-coil domain through the

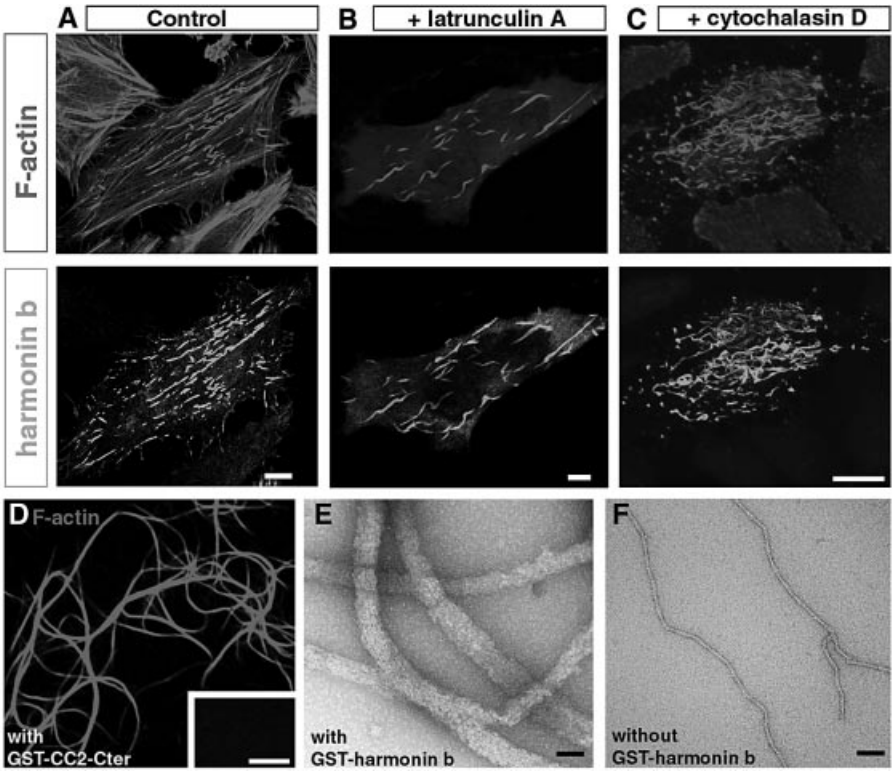

Fig. 3. (A–C) Harmonin b induces a resistance of actin filament to latrunculin A and cytochalasin D. (**A**) Transfected HeLa cells labelled for F-actin (red) and harmonin b (green). Actin stress fibres are observed in transfected cells that produce harmonin b as well as in the surrounding untransfected cells. (B and C) The disruptive effect of latrunculin A (**B**) and cytochalasin D (**C**) on actin filaments is not observed in transfected cells that produce harmonin b. With either of these drugs, both the cortical actin filaments and the harmonin b-unlabelled stress fibres were disrupted, whereas the harmonin b-associated actin fibres were unaffected. (D–F) Harmonin b is an actin-bundling protein. Light microscopy (E) and electron microscopy (F and G) demonstration of F-actin bundle formation. (**D**) In the presence of GST-tagged CC2-Cter harmonin fragment, large and long F-actin bundles are observed. No bundled F-actin is observed in the absence of this protein (inset in D). *In vitro* electron microscopy analysis showed that actin filaments assemble into bundles in the presence (**E**), but not in the absence (**F**) of harmonin b. Bars: 10 μm in (A–C), 5 μm in (D) and 60 nm in (E) and (F).

C-terminal end (CC2-Cter, amino acids 405–859) of the protein (not shown). In transfected cells, harmonin b-labelled structures were observed as either punctiform or long and curvy filaments (Figure 2B–D). Using three-dimensional spatial analysis, we found that the former are present almost exclusively at the cell plasma membrane–substrate interface, whereas the latter extended up to 10 μm throughout the cell, both being distinct from the actin stress fibres. We then studied the dynamics of green fluorescent protein (GFP)–harmonin b distribution in HeLa cells by digital fluorescence microscopy. The harmonin b label was first observed 6 h after transfection. At this stage, the protein was restricted to and highly concentrated at the distal end (barbed ends) of actin fibres, where they anchored to substrate adhesion sites (Figure 2E–J). Vinculin, a major component of the focal adhesion plaques (Zamir and Geiger, 2001) (Figure 2E, F and H–J), overlapped with the distal part of the harmonin b staining (Figure 2H and I). Observations performed at different intervals from 8 to 48 h after transfection indicated that harmonin b label extended further from the focal adhesion sites forming the long and curvy bundles. However, this changing pattern was slow as we observed only moderate modification of harmonin b-labelled structures in cells analysed by time lapse during a 4 h interval (not shown). To characterize further the behaviour of actin filaments in the presence of harmonin b, cells were treated with either latrunculin A (Figure 3B), which binds to and sequesters actin monomers, or cytochalasin D (Figure 3C), that binds to the barbed end of actin filaments and alters actin polymerization. With either of these drugs, both the cortical actin filaments and the stress fibres were disrupted, whereas the curvy, harmonin b-bound, actin filaments were unaffected (Figure 3A–C). Together, these results suggest that harmonin b stabilizes the actin filaments.

To determine how harmonin b interacts with F-actin, we then carried out *in vitro* binding assays (see Materials and methods). Harmonin b and rhodamine–phalloidin-labelled actin filaments were incubated together, and samples were visualized by light microscopy or were negatively stained for electron microscopy. We found that in the presence of the GST-tagged CC2-Cter harmonin b fragment (Figure 3D) or harmonin b (Figure 3E and F), actin filaments collected into large bundles. Upon GST cleavage by thrombin, the CC2-Cter harmonin b fragment also promoted F-actin bundling (Supplementary figure 3A). This actin-bundling activity of harmonin b was not affected by a high calcium concentration (10 mM) or calcium chelating agents (10 mM EGTA) (not shown). To determine whether harmonin b associates with these actin bundles, we mixed the GST-tagged CC2-Cter harmonin b fragment with actin filaments to allow bundling, then the bundles were separated from soluble proteins and single

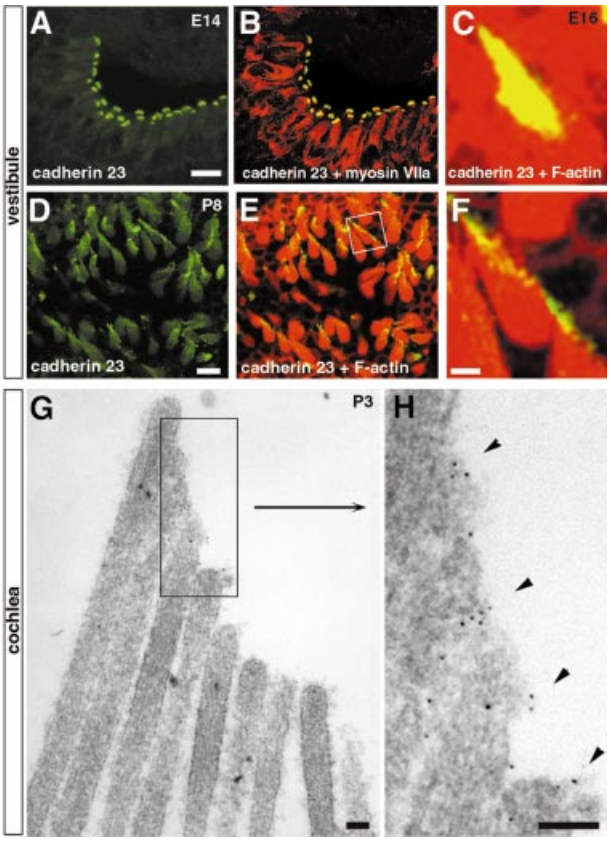

Fig. 4. Cadherin 23 in the differentiating hair cells (mouse). (**A** and **B**) In the vestibule, at E14, cadherin 23 is only detected at the apical surface of the hair cells (A), whereas myosin VIIa is detected in the entire hair cells (B). Up to E16, cadherin 23 delineates the entire length of the hair bundle, as shown by double staining for cadherin 23 and F-actin (**C**). (**D–F**) In a tangential section of a P8 vestibular macula, cadherin 23 (green) is also detected in the hair bundles, mainly at the tips of the stereocilia, visualized by F-actin staining (red). (**G** and **H**) Electron microscopy of a hair bundle from a P3 mouse cochlear hair cell. Cadherin 23 is detected between adjacent stereocilia, especially at their apical ends, as shown at higher magnification (arrowheads in H). Bars: 20 μm in (A) and (B); 3 μm in (C); 10 μm in (D); and (E), 5 μm in (F) and 100 nm in (G) and (H).

actin filaments by low-speed centrifugation. In the presence of the GST–CC2-Cter harmonin, the vast majority of F-actin was recovered in the pellet (Supplementary figure 3B). Finally, we demonstrated the direct binding of the CC2-Cter harmonin b fragment to F-actin by using CC2-Cter- or GST-coated beads incubated with actin filaments (Supplementary figure 3C and D). These results demonstrate that harmonin b has an actin-bundling activity that is independent of calcium.

Cadherin 23 is present in the stereocilia and binds to harmonin b

Mutations of the gene encoding cadherin 23 cause USH1D in man. To study the distribution of cadherin 23 in the mouse developing inner ear, we raised three polyclonal antibodies against extracellular or intracellular regions of the protein (see Materials and methods). Just like harmonin b, cadherin 23 was detected along the entire stereocilia as soon as they emerge, and subsequently became restricted to their apical regions (Figure 4A–F), as confirmed by immunoelectron microscopy on P3 cochlear hair cells (Figure 4G and H). Both in the vestibule and in the cochlea, the temporal pattern was also identical to that of harmonin b. From P30, cadherin 23 was no longer detected in the cochlear stereocilia and only persisted in a few vestibular type I and type II hair cells. The disappearance of cadherin 23 from the stereocilia of adult mice indicates that the protein is not a component of the apical links of mature hair bundles.

The similar spatio-temporal distributions of harmonin b and cadherin 23 in the stereocilia suggested that these molecules may interact. We therefore examined whether such an interaction could be detected in co-transfected HeLa cells (Figure 5). In cells producing the cadherin 23 cytodomain (amino acids 3086–3354) and harmonin b, the two proteins entirely co-localized throughout the cell cytoplasm (not shown). To determine whether cadherin 23 could recruit harmonin b to the cell membrane, we analysed its distribution in the presence of the hEcad–cad23 chimeric protein. The hEcad–cad23 protein is composed of the extracellular and transmembrane domains of Ecadherin directly linked to the cytodomain of cadherin 23 (Figure 5A). In HeLa cells producing the two proteins, the hEcad–cad23 chimera was detected at the cell–cell contacts, where it recruited harmonin b. In contrast, harmonin b was absent at cell–cell contacts lacking the hEcad–cad23 chimera (Figure 5B). Moreover, the presence of hEcad–cad23 modified the harmonin b–actin pattern, i.e. long harmonin b-bound curvy filaments changed into punctate labelled structures (Figure 5B; Supplementary figure 5), thus suggesting an association between harmonin b and cadherin 23. Pull-down assays were then performed. Extracts of transfected HEK293 cells producing either harmonin a, harmonin b or the myosin VIIa tail (amino acids 848–2215) were incubated with immobilized GST-tagged cadherin 23 cytodomain (amino acids 3086–3354) or GST alone. Harmonins a and b were recovered with the GST-tagged cadherin 23 cytodomain, but not with GST alone. In contrast, the myosin VIIa tail was not recovered (Figure 6A). The interaction between cadherin 23 and harmonin was analysed further by an *in vitro* binding assay (Figure 6B). Different harmonin fragments were produced (see Materials and methods) and incubated with immobilized biotin-tagged cadherin 23 cytodomain. Both the PDZ1–PDZ2 peptide (amino acids 138–403) of harmonin and the PDZ2 domain alone (amino acids 189–307) bound to the cadherin 23 cytodomain, whereas binding was not observed with either PDZ1 or PDZ3 (Figure 6B and E).

These findings were confirmed by the results of a yeast two-hybrid screening. The last 268 amino acids of the cadherin 23 cytoplasmic domain were used as a bait to screen exhaustively a P2–P6 inner ear sensory epithelium cDNA library. Eighteen independent clones encoding harmonin were found to bind specifically to the cadherin 23 cytodomain. The overlapping sequences of these clones, amino acids 114–322, map to the PDZ1 and PDZ2 domains of harmonin (Supplementary figure 6A). Together, these results demonstrate that harmonin, via its PDZ2 domain, binds to cadherin 23.

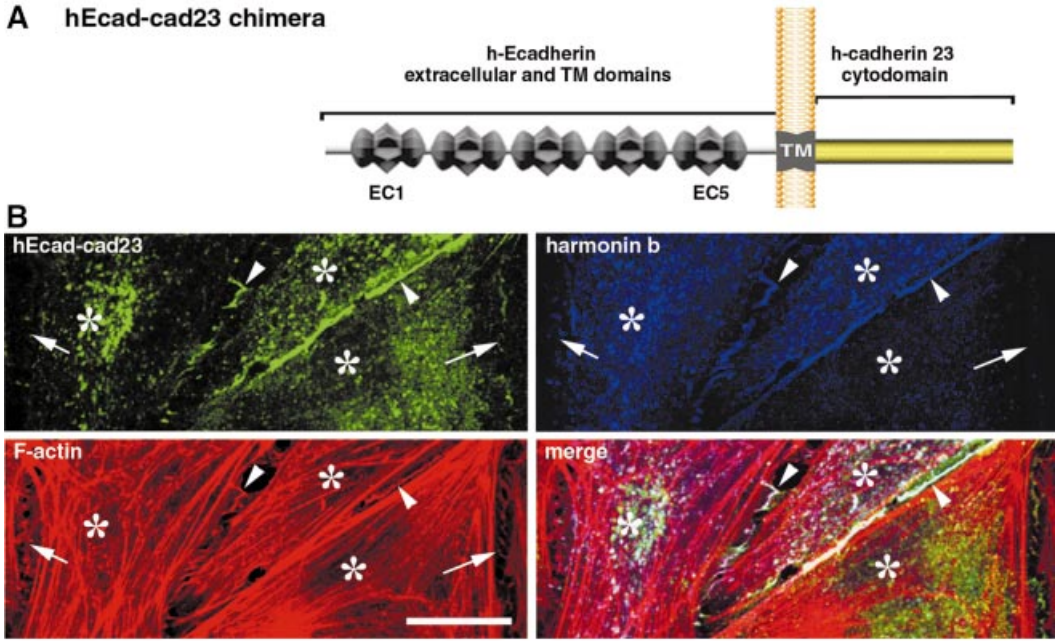

Fig. 5. Harmonin b co-localizes with hEcad–cad23 in co-transfected HeLa cells. (**A**) Schematic diagram of the hEcad–cad23 chimera: it is composed of the five extracellular cadherin repeats (EC) and the transmembrane domain (TM) of human Ecadherin (hEcad) fused to the human cadherin 23 cytodomain (cad23). (**B**) HeLa cells were transiently transfected with either hEcad–cad23 or harmonin b cDNAs for 20 h. The hEcad–cad23 chimeric protein is targeted to cell–cell contacts (green; revealed by Pcad-C) essentially at the junctions between two transfected cells (arrowheads). Harmonin b (V5-tagged) is also recruited to these contacts, where it co-localized with the hEcad–cad23 chimera and with actin filaments (red). Neither the hEcad–cad23 chimera nor harmonin b is enriched at cell–cell contacts established with untransfected cells (arrows). In the cell cytoplasm, the presence of the hEcad–cad23 protein shifts the filamentous pattern usually observed with harmonin b, to punctiform actin-rich structures. Asterisks indicate HeLa cell bodies. Bar: 20 μm.

Harmonin b binds to myosin VIIa and is mislocated in myosin VIIa-deficient mice

Myosin VIIa was recently shown to be a bona fide motor protein that moves along actin filaments (Udovichenko *et al*., 2002). Although the directionality of myosin VIIa movement along actin filaments has not been determined, all myosins (except for myosins VI and IXb) tested to date are actin plus end directed (Berg *et al*., 2001; Inoue *et al*., 2002). We thus addressed the possibility that myosin VIIa tows proteins towards the plus ends of actin filaments near the stereocilium tip. To this end, we studied the distribution of cadherin 23 and harmonin b in Myo7a^{4626SB} *shaker-1* mice which carry a premature stop codon in the motor domain of myosin VIIa, and have severely disorganized hair bundles (Mburu *et al*., 1997). In both the vestibular (Figure 7A–C, G and H) and cochlear (Figure 7D–F and I–K) hair cells from E20 to P30, we failed to detect harmonin b in the stereocilia. Instead, harmonin b was found to be organized in a circle of bead-like foci located around the periphery of the cuticular plate (Figure 7A, H and I). In contrast, harmonin a/c (Figure 7F) and cadherin 23 (Figure 7J) were both present in the stereocilia and distributed as in wild-type mice. Likewise, two other proteins of the stereocilia, namely espin, an actin cross-linking protein (Zheng *et al*., 2000), and stereocilin, a protein of as yet unknown function (Verpy *et al*., 2001), were distributed normally throughout the length of the stereocilium in control and mutant mice (Figure 6K and data not shown). These results suggest that myosin VIIa is involved in the transport of harmonin b up to the tip region of the stereocilium.

Such a proposal implies that the myosin VIIa tail and harmonin b physically interact. In co-transfected HeLa cells producing harmonin b and either the entire myosin VIIa tail or its C-terminal MyTH4 + FERM repeat (amino acids 1750–2215), we observed that the myosin VIIa fragments entirely co-localized with harmonin b and actin (Supplementary figure 6B; data not shown). Moreover, the presence of the myosin VIIa fragments profoundly modified the harmonin b–actin pattern, just as the cadherin 23 cytodomain did. Similar co-transfection experiments with harmonin a or c led to similar results, thus arguing in favour of an interaction of the three harmonin subclasses with myosin VIIa (data not shown). Because purified harmonin b was not stable, we tested the binding of harmonin a to myosin VIIa by *in vitro* binding assays. The C-terminal MyTH4 + FERM repeat of myosin VIIa did interact with GST-tagged harmonin a, and with GST–MyRIP (myosin VIIa and Rab-interacting protein) used as a positive control (El-Amraoui *et al*., 2002)), whereas it failed to bind to GST alone (Figure 6C) or GST-tagged cadherin 23 cytodomain (not shown). In contrast, the ezrin FERM domain did not bind to GST–harmonin a (Figure 6C). By using various constructs expressing PDZ domains of harmonin b, we showed that only PDZ1 has affinity for myosin VIIa (Figure 6D and E).

A yeast two-hybrid screen corroborated these results. Using a C-terminal fragment of the myosin VIIa tail containing the SH3, MyTH4 and FERM domains (amino acids 1605–2215) as the bait, six independent clones encoding harmonin were isolated from our inner ear two-hybrid cDNA library. Their overlapping sequences encode

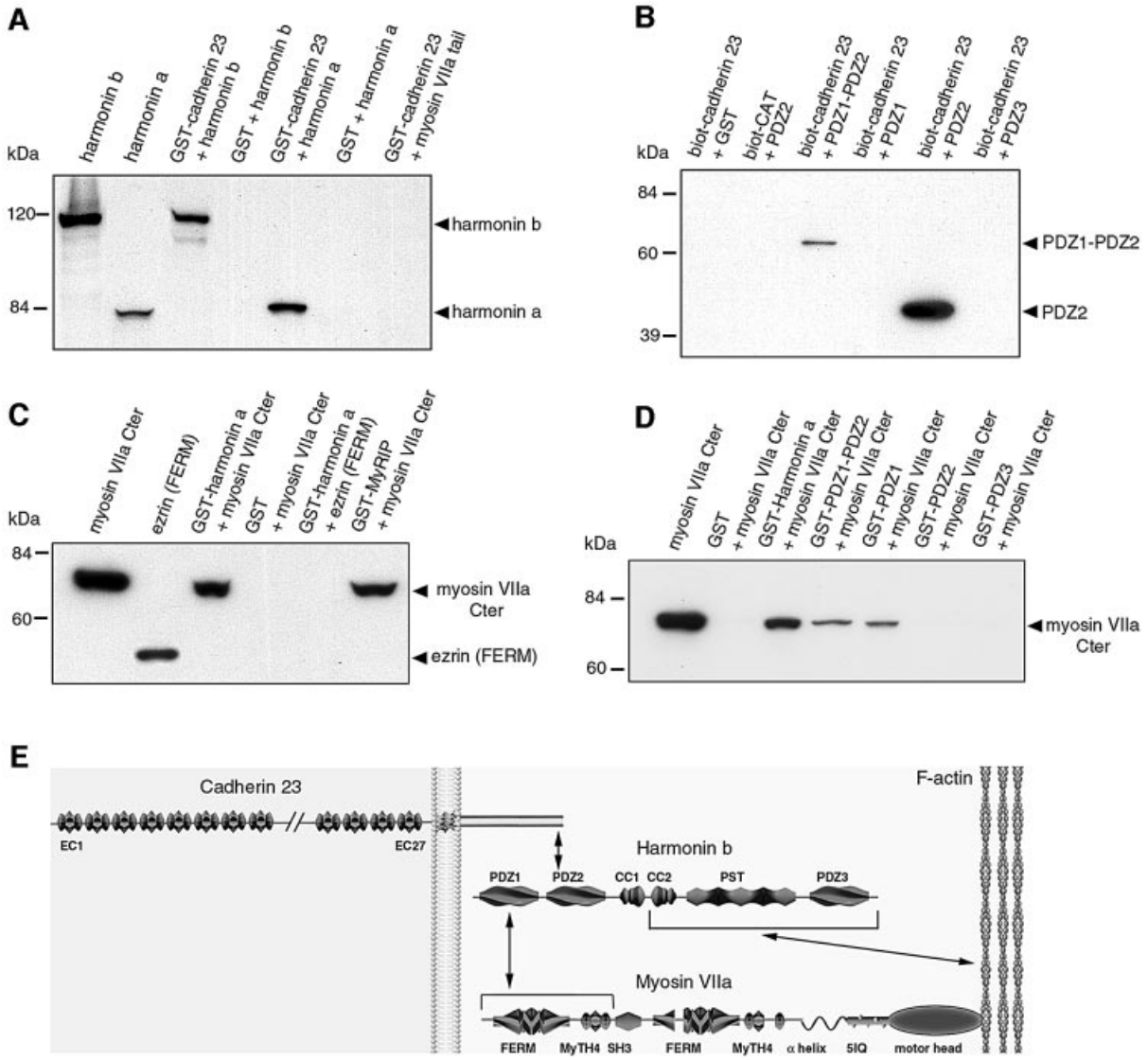

Fig. 6. Harmonin binds to cadherin 23 and myosin VIIa. (**A**) Pull-down assay. Extracts of transfected HEK293 cells producing either harmonin a, harmonin b or the myosin VIIa tail were incubated with immobilized GST-tagged cadherin 23 cytodomain or GST alone. The harmonins a and b bind to the GST-tagged cadherin 23 cytodomain but not to GST alone. The myosin VIIa tail does not bind to cadherin 23. (B–D) *In vitro* binding assays. (**B**) Characterization of the harmonin–cadherin 23 interaction domain. Different harmonin fragments were incubated with immobilized biotin-tagged cadherin 23 cytodomain. Only the PDZ1–PDZ2 peptide (amino acids 138–403) of harmonin and the PDZ2 domain alone (amino acids 189–307) bound to the cadherin 23 cytodomain. Biotin-tagged CAT (chloramphenicol acetyltransferase) was used as a negative control. (**C**) The C-terminal MyTH4 + FERM repeat of myosin VIIa (myosin VIIa-Cter) is incubated with different GST-tagged proteins. The myosin VIIa-Cter interacts with GST-tagged harmonin a, and with GST–MyRIP (used as a positive control), whereas it fails to bind to GST. The ezrin FERM domain (used as a negative control) does not bind to GST–harmonin a. (**D**) Characterization of the harmonin–myosin VIIa interaction domain. The myosin VIIa-Cter was incubated with different immobilized GST-tagged harmonin fragments. The PDZ1 domain of harmonin, but neither PDZ2 nor PDZ3, binds to myosin VIIa. (**E**) Schematic diagram illustrating how harmonin b could interact with myosin VIIa, cadherin 23 and F-actin. Acronyms: FERM (4.1, ezrin, radixin, moesin); MyTH4 (myosin tail homology 4); SH3 (src homology-3), IQ (isoleucine–glutamine motifs); EC (extracellular cadherin repeats).

a harmonin fragment (amino acids 90–368) containing PDZ1, PDZ2 and part of the CC1 domain (Supplementary figure 6C). Together, these results demonstrate that harmonin, via its PDZ1 domain, interacts with the myosin VIIa tail.

Discussion

In this study, we addressed the developmental role of harmonin in the inner ear sensory cells (hair cells). Mutations in the gene, *USH1C*, encoding this PDZ domain-containing protein have been shown to underlie one genetic form of USH1 (Bitner-Glindzicz *et al*., 2000; Verpy *et al*., 2000). Here, we show that harmonin directly interacts with cadherin 23, a protein defective in another genetic form of USH1 (Bolz *et al*., 2001; Bork *et al*., 2001). We also show that harmonin b, which thus far has only been detected in the inner ear (Verpy *et al*., 2000), binds to actin filaments. In addition, cadherin 23 and harmonin b concomitantly appear in the emerging stereocilia and disappear from the adult hair bundle. Together, these results strongly suggest that harmonin b bridges cadherin 23 to the cytoskeletal actin core of the stereocilium. Since *Cdh23* mutations result in the

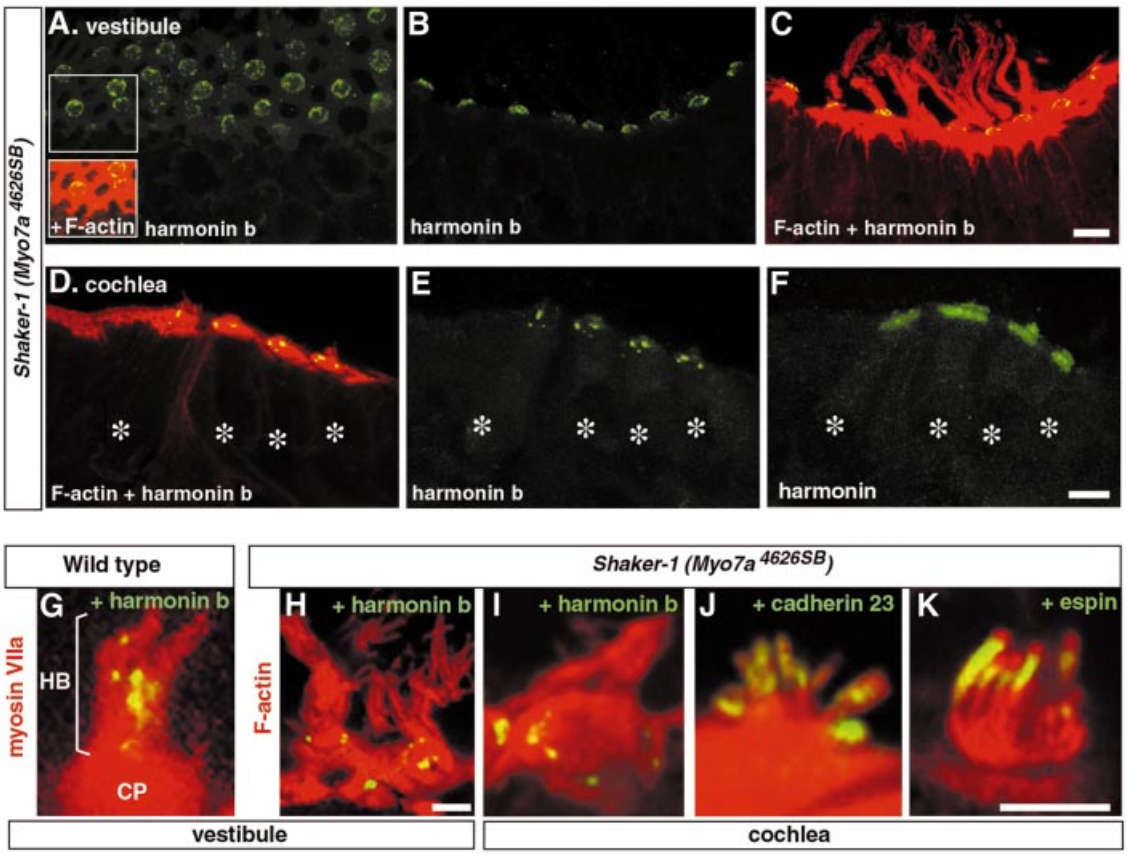

Fig. 7. Myosin VIIa is required for the proper targeting of harmonin b. Vestibular (A–C) and cochlear (D–F) hair cells from *shaker-1* Myo7a^{4626SB} mice at P6. (**A**–**C**) Harmonin b (green) decorates the apical surface of the hair cells, around the cuticular plate. Harmonin b is not detected in the hair bundles visualized by F-actin staining (red). (**D**–**F**) In the cochlea as well (asterisks over hair cell bodies), harmonin b fails to reach the hair bundle and punctiform harmonin b staining is observed around and within the hair cell cuticular plate (D and E). (F) In an adjacent section labelled with the NW2 antibody to harmonins a, b, and c, all harmonin isoforms are detected simultaneously. In addition to the harmonin b staining revealed in (E), a diffuse labelling corresponding to harmonins a and c is observed in the cuticular plate and the hair bundle as well. (G–K) Higher magnification views of vestibular (**G** and **H**) and cochlear (**I**–**K**) hair bundles from P2 mice. (G) In wild-type mice, myosin VIIa (red) is present throughout the cell, including the cuticular plate (CP) and the overlying hair bundle (HB). Harmonin b (yellow) is located mainly into the hair bundle. (H–K) In contrast, in *shaker-1* Myo7a^{4626SB} mice, harmonin b is organized mainly in a circle of bead-like foci located between the actin-rich cuticular plate and the actin of the circumferential belt (H and I), whereas cadherin 23 (J) and espin (K), a putative actin filament cross-linking protein of the stereocilia, are properly targeted to the hair bundle. Bars: 10 μm in (A–F); and 5 μm in (G–K).

disorganization of the hair bundle, and cadherin 23 is a member of the cadherin superfamily of cell–cell adhesion molecules, it has been proposed that this protein may cross-link the stereocilia (Di Palma *et al*., 2001). Here, we show that cadherin 23 is present at the surface of the growing stereocilia, whereas it is absent from the hair bundles of adult mice. Therefore, cadherin 23, via homophilic interaction, is likely to form transient lateral links that interconnect the stereocilia from their emergence up to their final maturation. As a consequence of its extended extracellular region (27 cadherin repeats) and as proposed for the related FAT cadherin (Cox *et al*., 2000), cadherin 23 may also function as a sensor that detects cell membrane proximity in its microenvironment. Thereby, cadherin 23 could initiate contact between adjacent stereocilia.

The extracellular region of classical cadherins (e.g. Ecadherin) consists of five repeats. Adhesion between neighbouring cells is mediated by the homophilic interaction of the cadherin extracellular domains that form dimers *in trans*, and cluster, in a calcium-dependent manner (Angst *et al*., 2001; Jamora and Fuchs, 2002). Ecadherins only provide weak cell–cell adhesion unless they are bridged to the actin cytoskeleton. The formation of adherens junctions involves the dynamic and regulated assembly of its molecular components (Gumbiner, 2000; Angst *et al*., 2001; Jamora and Fuchs, 2002). The cytodomain of Ecadherin binds to β-catenin, which recruits α-catenin that interacts with actin filaments (Yap *et al*., 1997; Imamura *et al*., 1999). The α- and β-catenins are actually absent from the growing hair bundle (A.El-Amraoui, unpublished results). Furthermore, cadherin 23 lacks the consensus R1 and R2 binding sites for β-catenin (Imamura *et al*., 1999) but possesses the C-terminal tripeptide class 1 consensus binding site for a PDZ domain, S/T-X-Φ (where X is any amino acid and Φ is hydrophobic) (Sheng and Sala, 2001). Further studies are required to determine whether cadherin 23 binding to harmonin is mediated through this C-terminal tripeptide (TEL). Our results reveal a novel mode of association between a member of the cadherin family and the cytoskeleton, via the binding of the cadherin cytodomain to a PDZ domain-containing protein, harmonin b, that directly interacts with F-actin. The cadherin

23–harmonin b–actin filament complex is expected to strengthen the cohesion between stereocilia, by anchoring cadherin 23 to the actin core, initially along the entire length of the growing stereocilia and eventually in the more mature hair bundle, at discrete apical sites. In addition, the F-actin-bundling property of harmonin b that we show *in vitro* suggests that harmonin b is implicated in the dynamics of the stereocilia actin core in the developing hair bundle. Two other actin-bundling proteins, fimbrin and espin, have been identified in the stereocilia (Drenckhahn *et al*., 1991; Zheng *et al*., 2000). However, unlike harmonin b, they distribute along the entire stereocilium and are present both in the developing and the adult stereocilia. The actin-bundling activity of harmonin b, like that of espin and unlike that of fimbrin, is calcium independent. During hair bundle morphogenesis, harmonin b could contribute, as proposed for fimbrin and espin (Drenckhahn *et al*., 1991; Zheng *et al*., 2000), to the stiffness of the stereocilia. Moreover, harmonin b-bound actin filaments in HeLa cells exhibit a very unusual resistance to both cytochalasin D and latrunculin A, which suggests that harmonin b shifts the dynamics of actin filaments towards stabilization. Based on the dynamic expression pattern of harmonin b in the growing stereocilia, we propose that the protein stabilizes elongating actin filaments and, as growth ceases during late maturation, their barbed ends.

Our results also establish that myosin VIIa, an actin-based motor protein (Udovichenko *et al*., 2002) which is defective in still another genetic form of USH1 (Weil *et al*., 1995), binds to harmonin *in vitro*. In *shaker-1* Myo7a^{4626SB} mice with severely disorganized hair bundles, harmonin b is absent from the stereocilia. In these mutants, harmonin b remains associated with the periphery of the cuticular plate, where it may be associated with the actin filaments that make up this structure. Remarkably, this pattern is reminiscent of that observed transiently in normal development when the hair bundle starts growing (see insets Figure 1D). Therefore, in wild-type mice, myosin VIIa is likely to be involved in the transport of harmonin b into the stereocilia up to its final location. We have shown previously that myosin VIIa binds to vezatin, a transmembrane protein of the hair bundle, which is closely associated with the ankle links (a subset of lateral links that interconnect the bases of adjacent stereocilia), and proposed that myosin VIIa, via its interaction with vezatin, acts locally to create a tension force between the actin core and the plasma membrane of the stereocilia; the same role would apply to the cell–cell junction where both myosin VIIa and vezatin are located (Kussel-Andermann *et al*., 2000) as well as harmonin and cadherin 23 (data not shown). Based on this proposed function for the myosin VIIa–vezatin interaction, the abnormal gating of the mechanotransduction channels which has been detected in *shaker-1* Myo7a^{4626SB} mice has been suggested to result from the defect of the force myosin VIIa may apply to the transduction channel (Kros *et al*., 2002). An alternative hypothesis should now be considered, namely that myosin VIIa indirectly modulates the gating properties of the channel by translocating regulatory proteins of the transduction process to the tip of the stereocilium. It is noteworthy that, unlike harmonin b, harmonins a and c were found along the entire length of the stereocilia even in the absence of myosin VIIa, thus indicating that myosin VIIa is dispensable for the transport of these isoforms into the stereocilia.

From the present functional characterization of harmonin b, cadherin 23 and myosin VIIa, we propose the following molecular scenario in the developing hair bundle. Myosin VIIa first conveys harmonin b to its stereociliar location. There, harmonin b anchors cadherin 23-containing interstereociliar links to the actin filament cores of growing stereocilia. In this respect, one should recall that at early stages of hair bundle development, the stereocilia do not have the actin rootlets that eventually anchor into the cuticular plate and are thought to contribute to bundle stability (Tilney *et al*., 1983). We suggest that the earliest connections between growing stereocilia are critical for shaping the hair bundle as a coherent unit, and that this relies on a cooperation between the three aforementioned proteins. A failure in this process would lead to the hair bundle disorganization observed in USH1 mouse models. Finally, an attractive hypothesis is that the functional network formed by harmonin b, cadherin 23 and myosin VIIa also implicates the proteins defective in the other genetic forms of USH1.

Materials and methods

Yeast two-hybrid screenings

Microdissected vestibular sensory epithelia of 292 mice (aged from P2 to P6) were used to generate a random-primed cDNA library (Rain *et al*., 2001). Screenings were performed using two different baits: the intracellular region of cadherin 23 (amino acids 3086–3354) and the C-terminal fragment of myosin VIIa tail (amino acids 1562–2215), composed of SH3, MyTH4 and FERM domains.

Expression constructs

A cDNA encoding the cytoplasmic region of cadherin 23 (NM-022124; amino acids 3086–3354) was obtained by RACE-PCR on a human retinal Marathon-cDNA library. PCR products were subcloned into pCMV-tag3B (Myc tag, Stratagene) and pcDNA (No tag, Invitrogen) for expression in HeLa cells, and into pGex-4T1 (GST tag, Amersham) and pXa3 (biotin tag, Promega) for protein production. The mouse full-length cDNAs encoding harmonin isoforms a1 (AF228924; amino acids 1–548), b2 (AY103465; 1–859) and c1 (1–403) were amplified from the inner ear cDNA library as a template and cloned into pCMV-tag3C, pcDNA and pGex-4T1. cDNAs encoding harmonin truncated forms, i.e. PDZ1–PDZ2 (amino acids 72–307), PDZ1 (72–88), PDZ2 (189–307) and PDZ3 (738–849), were subcloned into pCMV-tag3C and pGex-4T1. A human cDNA encoding the myosin VIIa tail (amino acids 847–2215) was cloned in pcDNA for expression in HeLa cells. For protein production, a zebrafish cDNA encoding His-tagged myosin VIIa C-terminal tail fragment (88.5% amino acid identity with the corresponding human fragment) was subcloned in the pFastBac HTa vector (baculovirus system, Life Technologies). hEcad–cad23 is a chimeric protein derived from two plasmids: (i) pcDNA3/hEcad-Cαctn, provided by M.Lecuit (Institut Pasteur), in which the extracellular and transmembrane domains of human Ecadherin (hEcad) are fused to the C-terminal 398 amino acids of α-catenin (Cαctn); and (ii) pCMV-cad23 containing the human cadherin 23 cytodomain (amino acids 3086–3354). The pcDNA3/hEcad-Cαctn plasmid was digested by *Cla*I and *Xba*I to eliminate the α-catenin fragment (all 398 amino acids). This fragment was then replaced by an amplified *Cla*I–*Xba*I fragment encoding the human cadherin 23 cytodomain (cad23; amino acids 3087–3354), thus giving rise to pcDNA3/hEcad–cad23.

Antibody production

The H3 polyclonal antibody was generated against a bacterially expressed peptide common to the three harmonin subclasses (PH3; amino acids 1–89). The H1b and H2b antibodies to harmonin b were generated against an epitope located in the PST domain of the protein (PHb: RTGDPGHPADDWEA; amino acids 636–649). Three different rabbit

polyclonal antibodies against human cadherin 23 were generated: cad-C against a peptide in the cadherin 23 cytodomain (Pcad-C; amino acids 3324–3339), cad-N against two peptides in the extracellular region, namely Pcad-N1 (amino acids 1161–1174) and Pcad-N2 (amino acids 2456–2470), and cad-CN against all three peptides.

The specificity of the affinity-purified antibodies was assayed by immunofluorescence and immunoblot analysis. Substitution of the pre-immune sera for the purified anti-harmonin or anti-cadherin 23 antibody and pre-adsorption of the antibodies with the corresponding antigens were used as negative controls.

Pull-down and in vitro binding experiments

Transient transfections of HEK293 cells were performed using PolyFect Transfection Reagent (Qiagen) following the manufacturer's instructions. Cells were collected 2 days after transfection and processed for pull-down experiments as described (Kussel-Andermann *et al*., 2000). The *in vitro* binding assays were performed using glutathione–Sepharose (Amersham), or Tetra-link avidin resins (Promega) as described (Kussel-Andermann *et al*., 2000). Briefly, to test harmonin–myosin VIIa interaction, a bacterial lysate containing the GST–harmonin fusion protein was incubated with glutathione–resin for 90 min at 4°C. The resins were washed with binding buffer (phosphate-buffered saline with 5% glycerol, 5 mM $MgCl_2$ and 0.1% Triton X-100) supplemented with a protease inhibitor cocktail (Roche), and then incubated with the His-tagged myosin VIIa, or a His-tagged control protein, ezrin (amino acids 1–309) for 2 h at 4°C. The resins were washed four times with binding buffer supplemented with 150 mM NaCl, and bound proteins were analysed by SDS–PAGE and immunoblotting, using the enhanced chemiluminescence (ECL) system (Amersham).

Immunofluorescence and electron microscopy analysis

HeLa cell lines were cultivated in 10% fetal calf serum (FCS)-supplemented Dulbecco's modified Eagle's medium (DMEM). Transient transfections of these cells were performed using Effectene (Qiagen). Immunohistofluorescence analysis was carried out on fixed cells and cryostat sections of inner ears, as described (Kussel-Andermann *et al*., 2000). Cells and tissue sections were analysed with a laser scanning confocal microscope (LSM-510, Zeiss). For immunoelectron microscopy, cochleas from P3 mice (CD1 strain) were labelled with affinity-purified cad-N anti-cadherin 23 antibodies or, as a control, non-immune rabbit IgG (Goodyear and Richardson, 1999).

The following mouse monoclonal antibodies were used: anti-Myc (clone 9E10) and anti-His (Santa Cruz); anti-GST (Amersham); anti-vinculin (Sigma); and anti-V5 (Invitrogen). For myosin VIIa detection in western blots, and harmonin–myosin VIIa double labelling experiments, a monoclonal mouse antibody (Farida-Nato, IP), raised against a human myosin VIIa tail fragment (U39226; amino acids 905–1032), was used. Several polyclonal rabbit antibodies were used, which were directed against myosin VIIa (SSI) (El-Amraoui *et al*., 1996), harmonin (NW2) (Kobayashi *et al*., 1999), espin (Zheng *et al*., 2000) and stereocilin (Verpy *et al*., 2001).

Actin binding assays

A 50 μM G-actin solution (Molecular Probes) was polymerized by incubation for 30 min at 37°C in a high salt buffer containing 50 mM KCl and 2 mM $MgCl_2$. A 10 μg aliquot of GST–harmonin b or GST–CC2-Cter truncated form was incubated for 30 min with 15 μl of 10 μM F-actin reconstituted from actin powder at 37°C. Actin polymers were either labelled with rhodamine–phalloidin and then observed under a fluorescence microscope, or analysed by electron microscopy after negative staining (Harris, 1991). Co-sedimentation assays were done by mixing GST–CC2-Cter harmonin b fragment with F-actin, followed by centrifugation (30 min, 13 000 *g*). The same amounts of supernatant and pellet fractions were subjected to SDS–PAGE and analysed with the H1b anti-harmonin antibody and Coomassie blue staining. For direct binding, glutathione–Sepharose beads coupled with GST or GST–CC2-Cter harmonin b truncated form were mixed with 10 μM bundled F-actin (F-actin mix supplemented with 50 mM $MgCl_2$). After three washes in high salt buffer, F-actin was then visualized using rhodamine–phallodin.

Animals

Wistar Rats and RJ Swiss mice (Janvier, France) were used. Embryonic day 0 (E0) was determined by vaginal plug detection, and the day of birth was P0. The *shaker-1* Myo7a^{4626SB} mice, obtained by ethylnitrosourea (ENU) mutagenesis, were kindly provided by Dr K.Steel (MRC, UK). Mice were genotyped as described (Self *et al*., 1998), and the absence of myosin VIIa was confirmed by immunohistochemistry using the anti-myosin VIIa antibody. Twenty mutant mice at E20, P0, P2, P6, P10, P25, P30 and P60, with the same numbers of littermate controls, were analysed.

Supplementary data

Supplementary data are available at *The EMBO Journal* Online.

Acknowledgements

We thank J-P.Hardelin, P.Cossart and P.Herbomel for critical reading of the manuscript, J.Levilliers and D.Weil for their inexhaustible help, S.Ernest and M.Lecuit for the zebrafish myosin VIIa and hEcad–Cαctn chimeric constructs, and J.Bartles and I.Kobayashi for their kind gift of the anti-espin and anti-harmonin antibodies, respectively. This work was supported by grants from the EC (QLG2-CT-1999-00988), the R. and G.Strittmatter Foundation, Retina-France, the A. and M.Suchert, Forschung contra Blindheit—Initiative Usher Syndrom, Deutsche Forschungsgemeinschaft (Wo 548/3 and 4; U.W.), FAUN-Stiftung (U.W.), Pinguin Stiftung (K.R.F. and U.W.) and The Wellcome Trust (057410/Z/99Z; G.R.). The confocal microscope was purchased with a donation from Marcel and Liliane Pollack. B.B. has a fellowship from Fondation pour la Recherche Médicale (France).

References

Ahmed,Z.M., Riazuddin,S., Bernstein,S.L., Ahmed,Z., Khan,S., Griffith,A.J., Morell,R.J., Friedman,T.B. and Wilcox,E.R. (2001) Mutations of the protocadherin gene PCDH15 cause Usher syndrome type 1F. *Am. J. Hum. Genet.*, **69**, 25–34.

Alagramam,K.N. *et al*. (2001a) Mutations in the novel protocadherin *PCDH15* cause Usher syndrome type 1F. *Hum. Mol. Genet.*, **10**, 1709–1718.

Alagramam,K.N., Murcia,C.L., Kwon,H.Y., Pawlowski,K.S., Wright,C.G. and Woychik,R.P. (2001b) The mouse Ames waltzer hearing-loss mutant is caused by mutation of Pcdh15, a novel protocadherin gene. *Nat. Genet.*, **27**, 99–102.

Angst,B.D., Marcozzi,C. and Magee,A.I. (2001) The cadherin superfamily. *J. Cell Sci.*, **114**, 625–626.

Berg,J.S., Powell,B.C. and Cheney,R.E. (2001) A millennial myosin census. *Mol. Biol. Cell*, **12**, 780–794.

Bitner-Glindzicz,M. *et al*. (2000) A recessive contiguous gene deletion causing infantile hyperinsulinism, enteropathy and deafness identifies the Usher type 1C gene. *Nat. Genet.*, **26**, 56–60.

Bolz,H. *et al*. (2001) Mutation of CDH23, encoding a new member of the cadherin gene family, causes Usher syndrome type 1D. *Nat. Genet.*, **27**, 108–112.

Bork,J.M. *et al*. (2001) Usher syndrome 1D and nonsyndromic autosomal recessive deafness DFNB12 are caused by allelic mutations of the novel cadherin-like gene *CDH23*. *Am. J. Hum. Genet.*, **68**, 26–37.

Cox,B., Hadjantonakis,A.K., Collins,J.E. and Magee,A.I. (2000) Cloning and expression throughout mouse development of *mfat1*, a homologue of the *Drosophila* tumour suppressor gene *fat*. *Dev. Dyn.*, **217**, 233–240.

Denman-Johnson,K. and Forge,A. (1999) Establishment of hair bundle polarity and orientation in the developing vestibular system of the mouse. *J. Neurocytol.*, **28**, 821–835.

DeRosier,D.J. and Tilney,L.G. (1989) The structure of the cuticular plate, an *in vivo* actin gel. *J. Cell Biol.*, **109**, 2853–2867.

DeRosier,D.J. and Tilney,L.G. (2000) F-actin bundles are derivatives of microvilli: what does this tell us about how bundles might form? *J. Cell Biol.*, **148**, 1–6.

DiPalma,F., Holme,R.H., Bryda,E.C., Belyantseva,I.A., Pellegrino,R., Kachar,B., Steel,K.P. and Noben-Trauth,K. (2001) Mutations in Cdh23, encoding a new type of cadherin, cause stereocilia disorganization in waltzer, the mouse model for Usher syndrome type 1D. *Nat. Genet.*, **27**, 103–107.

Drenckhahn,D., Engel,K., Hofer,D., Merte,C., Tilney,L. and Tilney,M. (1991) Three different actin filament assemblies occur in every hair cell: each contains a specific actin crosslinking protein. *J. Cell Biol.*, **112**, 641–651.

El-Amraoui,A., Sahly,I., Picaud,S., Sahel,J., Abitbol,M. and Petit,C. (1996) Human Usher 1B/mouse shaker-1: the retinal phenotype discrepancy explained by the presence/absence of myosin VIIA in the photoreceptor cells. *Hum. Mol. Genet.*, **5**, 1171–1178.

El-Amraoui,A., Schonn,J.S., Kussel-Andermann,P., Blanchard,S., Desnos,C., Henry,J.P., Wolfrum,U., Darchen,F. and Petit,C. (2002) MyRIP, a novel Rab effector, enables myosin VIIa recruitment to retinal melanosomes. *EMBO Rep.*, **3**, 463–470.

Gale,J.E., Marcotti,W., Kennedy,H.J., Kros,C.J. and Richardson,G.P. (2001) FM1-43 dye behaves as a permeant blocker of the hair-cell mechanotransducer channel. *J. Neurosci.*, **21**, 7013–7025.

Goodyear,R. and Richardson,G. (1999) The ankle-link antigen: an epitope sensitive to calcium chelation associated with the hair-cell surface and the calycal processes of photoreceptors. *J. Neurosci.*, **19**, 3761–3772.

Gumbiner,B.M. (2000) Regulation of cadherin adhesive activity. *J. Cell Biol.*, **148**, 399–404.

Harris,J.R. (1991) Negative staining-carbon film technique: new cellular and molecular applications. *J. Electron Microsc. Tech.*, **18**, 269–276.

Hudspeth,A.J. (1997) How hearing happens. *Neuron*, **19**, 947–950.

Imamura,Y., Itoh,M., Maeno,Y., Tsukita,S. and Nagafuchi,A. (1999) Functional domains of α-catenin required for the strong state of cadherin-based cell adhesion. *J. Cell Biol.*, **144**, 1311–1322.

Inoue,A., Saito,J., Ikebe,R. and Ikebe,M. (2002) Myosin IXb is a single-headed minus-end-directed processive motor. *Nat. Cell Biol.*, **4**, 302–306.

Jamora,C. and Fuchs,E. (2002) Intercellular adhesion, signalling and the cytoskeleton. *Nat. Cell Biol.*, **4**, 101–108.

Kobayashi,I. *et al*. (1999) Identification of an autoimmune enteropathy-related 75-kilodalton antigen. *Gastroenterology*, **117**, 823–830.

Kros,C.J., Marcotti,W., van Netten,S.M., Self,T.J., Libby,R.T., Brown,S.D., Richardson,G.P. and Steel,K.P. (2002) Reduced climbing and increased slipping adaptation in cochlear hair cells of mice with Myo7a mutations. *Nat. Neurosci.*, **5**, 41–47.

Kussel-Andermann,P., El-Amraoui,A., Safieddine,S., Nouaille,S., Perfettini,I., Lecuit,M., Cossart,P., Wolfrum,U. and Petit,C. (2000) Vezatin, a novel transmembrane protein, bridges myosin VIIA to the cadherin–catenins complex. *EMBO J.*, **19**, 6020–6029.

Mburu,P., Liu,X.Z., Walsh,J., Saw,D.,Jr, Cope,M.J., Gibson,F., Kendrick-Jones,J., Steel,K.P. and Brown,S.D. (1997) Mutation analysis of the mouse myosin VIIA deafness gene. *Genes Funct.*, **1**, 191–203.

Mustapha,M. *et al*. (2002) A novel locus for Usher syndrome type I, USH1G, maps to chromosome 17q24–25. *Hum. Genet.*, **110**, 348–350.

Nishida,Y., Rivolta,M.N. and Holley,M.C. (1998) Timed markers for the differentiation of the cuticular plate and stereocilia in hair cells from the mouse inner ear. *J. Comp. Neurol.*, **395**, 18–28.

Petit,C. (2001) Usher syndrome: from genetics to pathogenesis. *Annu. Rev. Genomics Hum. Genet.*, **2**, 271–297.

Pickles,J.O., Comis,S.D. and Osborne,M.P. (1984) Cross-links between stereocilia in the guinea pig organ of Corti and their possible relation to sensory transduction. *Hear. Res.*, **15**, 103–112.

Rain,J.C. *et al*. (2001) The protein–protein interaction map of *Helicobacter pylori*. *Nature*, **409**, 211–215.

Self,T., Mahony,M., Fleming,J., Walsh,J., Brown,S.D. and Steel,K.P. (1998) Shaker-1 mutations reveal roles for myosin VIIA in both development and function of cochlear hair cells. *Development*, **125**, 557–566.

Sheng,M. and Sala,C. (2001) PDZ domains and the organization of supramolecular complexes. *Annu. Rev. Neurosci.*, **24**, 1–29.

Tilney,L.G., Egelman,E.H., DeRosier,D.J. and Saunder,J.C. (1983) Actin filaments, stereocilia and hair cells of the bird cochlea. II. Packing of actin filaments in the stereocilia and in the cuticular plate and what happens to the organization when the stereocilia are bent. *J. Cell Biol.*, **96**, 822–834.

Tuxworth,R.I., Weber,I., Wessels,D., Addicks,G.C., Soll,D.R., Gerisch,G. and Titus,M.A. (2001) A role for myosin VII in dynamic cell adhesion. *Curr. Biol.*, **11**, 318–329.

Udovichenko,I.P., Gibbs,D. and Williams,D.S. (2002) Actin-based motor properties of native myosin VIIa. *J. Cell Sci.*, **115**, 445–450.

Verpy,E. *et al*. (2000) A defect in harmonin, a PDZ domain-containing protein expressed in the inner ear sensory hair cells, underlies Usher syndrome type 1C. *Nat. Genet.*, **26**, 51–55.

Verpy,E. *et al*. (2001) Mutations in a new gene encoding a protein of the hair bundle cause non-syndromic deafness at the DFNB16 locus. *Nat. Genet.*, **29**, 345–349.

Weil,D. *et al*. (1995) Defective myosin VIIA gene responsible for Usher syndrome type 1B. *Nature*, **374**, 60–61.

Yap,A.S., Brieher,W.M. and Gumbiner,B.M. (1997) Molecular and functional analysis of cadherin-based adherens junctions. *Annu. Rev. Cell. Dev. Biol.*, **13**, 119–146.

Zamir,E. and Geiger,B. (2001) Components of cell–matrix adhesions. *J. Cell Sci.*, **114**, 3577–3579.

Zheng,L., Sekerkova,G., Vranich,K., Tilney,L.G., Mugnaini,E. and Bartles,J.R. (2000) The deaf jerker mouse has a mutation in the gene encoding the espin actin-bundling proteins of hair cell stereocilia and lacks espins. *Cell*, **102**, 377–385.

Received August 19, 2002; revised and accepted October 30, 2002